

Ionic strength and solvent control over the physical structure, electronic properties and superquenching of conjugated polyelectrolytes

ALEX D. SMITH, CLIFTON KWANG-FU SHEN*, SEAN T. ROBERTS**,
ROGER HELGESON and BENJAMIN J. SCHWARTZ***

Department of Chemistry and Biochemistry, University of California, Los Angeles, Los Angeles, CA 90095-1569, USA

Received 27 March 2004; revised 8 June 2004

Abstract—In this paper, we investigate the photophysical properties of the conjugated polyelectrolyte poly(2-methoxy-5-propyloxy sulfonate phenylene vinylene) (MPS-PPV), dissolved in both water and DMSO as a function of the solution ionic strength. Dynamic light scattering indicates that MPS-PPV chains exist in a highly agglomerated conformation in both solvents, and that the size of the agglomerates depends on both the ionic strength and the charge of the counter-ion. Even though the degree of agglomeration is similar in the two solvents, we find that the fluorescence quantum yield of MPS-PPV in DMSO is nearly 100-times greater than that in water. Moreover, intensity-dependent femtosecond pump-probe experiments show that there is a significant degree of exciton–exciton annihilation in water but not in DMSO, suggesting that the MPS-PPV chromophores interact to form interchain electronic species that quench the emission in water. Given that the emission quenching properties depend sensitively on the chain conformation and degree of chromophore contact, we also explore the superquenching properties of MPS-PPV in the two solvents as a function of ionic strength. We find that superquenching may be either enhanced or diminished in either of the solvents *via* addition of simple salts, and we present a molecular picture to rationalize how the conformational properties of conjugated polyelectrolytes can be tuned to enhance their emissive behavior for sensing applications.

Keywords: Poly(2-methoxy-5-propyloxy sulfonate phenylene vinylene); photophysical properties; superquenching; ionic strength; solvent control; fluorescence; femtosecond pump-probe experiments.

*Present address: Department of Chemistry, Northwestern University, Evanston, IL 60208-3113, USA.

**Present address: Department of Chemistry, Massachusetts Institute of Technology, Cambridge, MA 02139-4307, USA.

***To whom correspondence should be addressed. E-mail: schwartz@chem.ucla.edu

INTRODUCTION

Conjugated polymers are plastic materials that are semiconducting because of their extended π conjugation along the polymer backbone. These materials are quite versatile in that their structures can be chemically tailored to provide desired optical or electronic properties [1–3]. Thus, conjugated polymers offer great promise as the active media in solution-processed (and, hence, low cost), flexible, and/or large-area optoelectronic devices such as light-emitting diodes (LEDs) and photovoltaic cells. Because of these potential applications, conjugated polymers have been the subject of a great deal of recent interest [4–6]. Despite this large amount of interest, there has been controversy over the nature of the electronic structure of conjugated polymers. We [7–13] and others [14–18] have argued that a significant fraction of this controversy results from the fact that the electronic properties of conjugated polymer films depend sensitively on their processing history. The differences in the literature can then be rationalized by noting that different groups tend to process their polymer samples in different ways, thereby leading to different results and conclusions [19].

Why do the electronic properties of conjugated polymer films depend so sensitively on their processing history? We believe that memory of the conformation of the polymer chains in solution persists through the spin-coating process and survives into the film [7, 19]. Thus, the local packing of the chains and overall morphology of conjugated polymer films are controlled by the choice of solvent and the concentration of the polymer solution from which the films are cast. For example, dynamic light scattering experiments on the conjugated polymer poly(2-methoxy 5-[2'-ethylhexyloxy]-*p*-phenylene vinylene) (MEH-PPV) have shown that the polymer chains take on different physical conformations in different solvents: in “good” solvents, such as chlorobenzene (CB), the chains take on an open and extended structure, whereas in “poor” solvents, such as tetrahydrofuran (THF), the chains form a much tighter coil [8]. When dissolved in good solvents, like CB, MEH-PPV has a red-shifted emission spectrum and low photoluminescence (PL) quantum yield [7], consistent with the idea that the conjugated segments on the more open chain coils can easily pack to form weakly emissive inter-chain species, such as excimers [13, 14, 20, 21] or aggregates [7, 8, 22, 23]. Moreover, LEDs with the active MEH-PPV layer cast from a good solvent like CB tend to have higher charge mobility but relatively low electroluminescence quantum efficiencies, which is also consistent with good contact of the π systems between polymer chains [7, 9]. MEH-PPV in poor solvents like THF, on the other hand, shows a more blue-shifted emission spectrum with higher PL quantum yield, and MEH-PPV LEDs based on films cast from THF show low charge mobility but high electroluminescence efficiency. All of these observations are consistent with the idea that the π electrons on tightly coiled conjugated polymer chains in poor solvents cannot easily come into good electrical contact [7–9]. Thus, the fact that spin-coating does not remove memory of the solution chain conformation makes semiconductor polymer device performance sensitive to the details of the solution processing conditions [19]. Given that

device behavior is so intimately connected to processing history, it is natural to investigate the possibilities of tailoring the processing conditions to enhance device performance.

In the MEH-PPV examples described above, the difference in average coil size for the polymer in CB and THF solutions was only approx. 40% [8], which does not provide a terribly large dynamic range of chain coil sizes with which to work. It is well known, however, that the conformation of polymers containing electrically charged groups can be controlled over a much broader range [24–27]: Polymers in which only a subset of the monomer repeat units are charged are known as ionomers, and polymers in which every repeat unit is charged are referred to as polyelectrolytes. It is also well known that charged polymers can change coil size, agglomerate or even undergo coil-to-rod phase transitions as solution properties, such as the ionic strength, are varied [24, 25, 27, 28]. Recently, we have explored the properties of a phenylene vinylene-based conjugated ionomer, and found that by controlling the degree of charging along the polymer backbone, we could change the polymer coil size in solution by over a factor of three [11, 12]. This enormous change in coil size, in turn, led to dramatic differences in both the photophysical properties and device behavior of films of this material [12]. In this paper, we turn our attention to controlling the conformation and electronic properties not of conjugated ionomers but of conjugated polyelectrolytes. Recently, several groups have reported the synthesis of conjugated polyelectrolytes based on both poly(phenylene vinylene) [29–31] (PPV) and poly(phenylene ethynylene) [31–36] (PPE), and there is a growing interest in the use of these materials in both explosive detection [34, 36] and biosensing applications [33, 37–43]. Most of the bio- and chemosensor work is based on the fact that conjugated polymers show an unusual amplification of fluorescence quenching [37, 40, 43]. The quenching mechanism typically consists of excited-state electron transfer from the conjugated polymer to an electron acceptor (the quencher), causing non-radiative decay of the polymer excited state. For such charge transfer to occur, the electron acceptor must be physically close to the excited polymer chromophore donor [44]. For conjugated polyelectrolytes, this proximity between the donor and acceptor usually occurs because the quencher and polymer form a ground-state complex (static quenching), since the excited-state lifetime of most conjugated polymers is too short for efficient quenching to occur by diffusion of the acceptor (dynamic quenching). If the conjugated polymer chain is coiled such that many of its chromophores can easily undergo Förster energy transfer to the complex, then a single quencher molecule in a complex can effectively quench the fluorescence of many chromophores: this type of quenching amplification is referred to as “superquenching” [37]. For sensor applications, a quencher with a strong affinity for the polymer fluorophore but an even stronger affinity for the analyte of interest is used. Thus, in the presence of the analyte, the polymer–quencher complex is broken and the emission from many polymer chromophores is turned on, providing a sensitive fluorescence assay to detect the presence of the analyte [33, 36, 37].

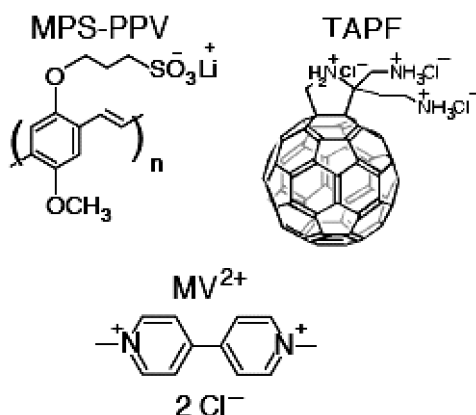
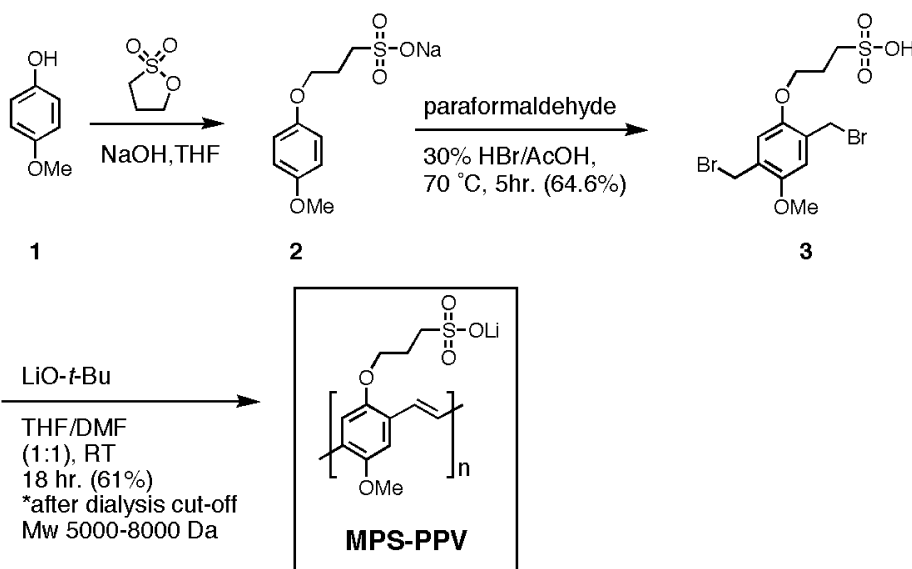


Figure 1. Chemical structures of the conjugated polyelectrolyte and quenchers used in this work. MPS-PPV (upper left), TAPF (upper right) and methyl viologen (MV²⁺, bottom).

Despite all this interest in sensing applications, there has yet to be a systematic study of how the conformation of conjugated polyelectrolytes (and, hence, their interaction with fluorescence quenchers) varies in different solution environments. Thus, in this paper, we present a preliminary exploration of how the conformation and superquenching properties of a water-soluble, PPV-based conjugated polyelectrolyte are controlled by factors such as choice of solvent, ionic strength, and counterion valency. The material we have chosen to study, poly(2-methoxy-5-propyloxy sulfonate phenylene vinylene) (MPS-PPV, see Fig. 1 for chemical structure), is the same one used in other studies [29, 30, 37, 38, 40, 42, 43], allowing us to make direct contact with much of the previous biosensing work. We find that MPS-PPV displays strikingly different optoelectronic properties in different solvent environments: for example, the fluorescence quantum yield of MPS-PPV is nearly 100-times stronger in DMSO than in water. Dynamic light scattering (DLS) suggests a physical agglomeration of the MPS-PPV chains in both solvents, and intensity-dependent photophysics experiments indicate that the MPS-PPV chromophores are aggregated in water but not in DMSO. We also investigate the superquenching properties of MPS-PPV in both water and DMSO at different ionic strengths. We find that the degree of superquenching changes dramatically in the presence of inert salts, even though the physical size of the agglomerated polymer chains undergoes relatively little change as the ionic strength is varied. Moreover, we also find that the degree of superquenching depends on both the solvent and the valency of the cation of the added salt. All of the results have important implications for the use of conjugated polyelectrolytes in optoelectronic or sensor applications.

EXPERIMENTAL

The synthesis of MPS-PPV is illustrated in Scheme 1. 4-Methoxyphenol **1** was converted to the corresponding sodium sulfonate by reacting with 1,3-propane



Scheme 1. Synthesis of MPS-PPV.

sultone in THF under basic conditions. The sodium salt **2** was obtained and then reacted with a mixture of paraformaldehyde and 30% HBr in acetic acid, while saturating the solution with HCl gas. The resulting precipitate **3** was collected and washed several times with a solution of 1,4-dioxane and diethylether. Spectrophotometric and mass spectrometric analyses of **3** were consistent with the proposed structure. The polymerization process was then carried out under Gilch conditions by adding LiOtBu into a solution (THF/DMF = 1:1) of **3**. After stirring at room temperature under argon for 16 h, dark-reddish MPS-PPV was obtained in 61% yield as crude product.

Upon completion of the polymerization, high-molecular-mass (MM) MPS-PPV (MM > 50 kDa) was separated from low-MM oligomers *via* serial dialysis with successively increasing exclusion molecular masses to remove shorter conjugation length/lower fluorescence quantum yield material. The importance of using multiple dialyses is illustrated in Fig. 2, which shows the absorption spectrum for material of MM > 5 kDa, as well as for MM > 50 kDa. The strong red shift and increased oscillator strength of the main exciton absorption band of the high-MM fraction indicates a material with a longer average π -conjugation length. Thus, we used only the high-MM (>50 kDa) fraction of our synthesized MPS-PPV for all the experiments reported below. Steady-state absorption experiments (including those in Fig. 2 above) were carried out on a Perkin-Elmer Lambda 25 UV-Vis Spectrometer. Steady-state fluorescence experiments were conducted on a JY-Horiba Fluorolog-3; photoluminescence quantum yields (PLQYs) of the conjugated polymer solutions were measured using Rhodamine 101G as a standard with assumed unity quantum yield and an approx. 0.05% detection limit. Dynamic light scattering (DLS) was

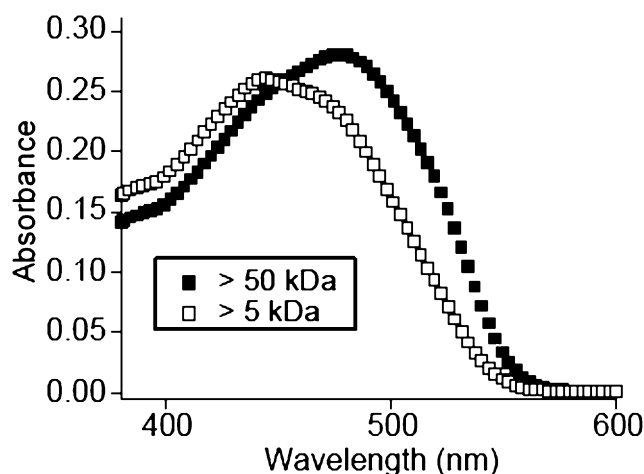
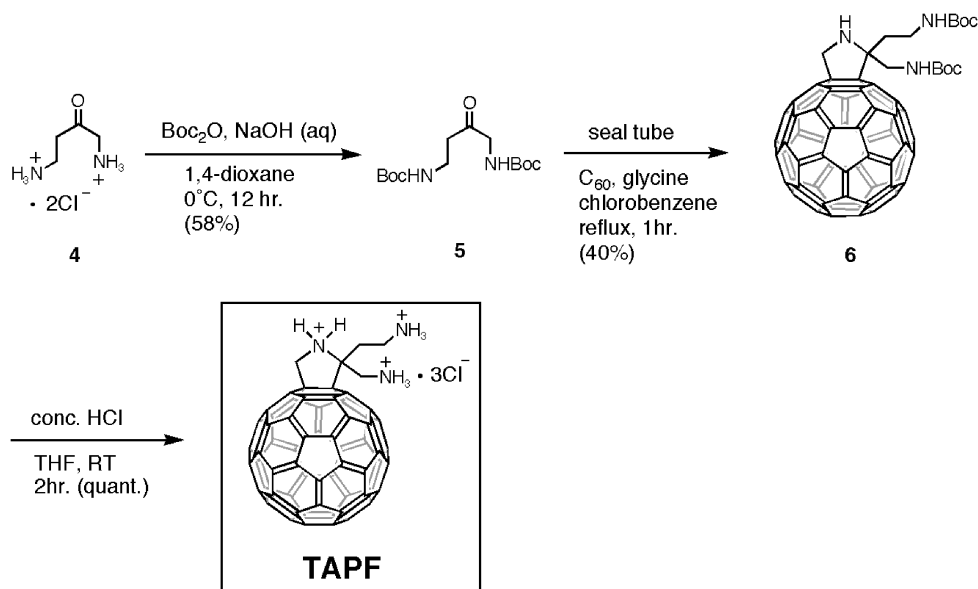


Figure 2. UV-Vis absorption spectrum of a 5 ppm solution of MPS-PPV in DMSO after dialysis to isolate the fraction of the material either with molecular mass > 5 kDa (open squares) or > 50 kDa (filled squares).

measured at 90° using a Coulter N4 Plus Submicron Particle Sizer. The results of the DLS experiments in water have a relative uncertainty better than $\pm 5\%$, but for DMSO the relative uncertainty is $\pm 15\%$ because the better index matching between MPS-PPV and DMSO results in a much poorer scattering efficiency. Femtosecond pump-probe transient absorption experiments were performed using an ultrafast spectrometer based on a regeneratively amplified Ti:Sapphire laser system that has been described completely elsewhere [7, 45].

For quenching experiments and experiments in which the ionic strength was varied, lithium chloride, calcium chloride and DMSO were obtained from Aldrich and used as received. Following the work of Chen *et al.* [37], we chose methyl viologen (MV^{2+} , see Fig. 1 for chemical structure) as a quencher that forms a strong static complex with MPS-PPV in water. Since MV^{2+} is not soluble in DMSO, however, we used a triamine-substituted fullerene derivative (triammonium pyrrolidinofullerene (TAPF), see Fig. 1 for chemical structure) as the quencher in our DMSO experiments. The synthesis of TAPF is summarized in Scheme 2. Commercially available 1,4-diammonium-butan-2-one hydrochloride **4** was protected by Boc_2O to afford ketone **5** in moderate yield. Subsequent Prato [3 + 2] cycloaddition to C_{60} with **5** in a sealed tube with glycine and chlorobenzene produced the fulleropyrrolidine adduct **6**. The two *t*-butyl carbamate groups on **6** were easily removed by stirring in conc. HCl and THF mixture for 2 h to afford TAPF quantitatively.

For all the experiments described in this paper, the MPS-PPV samples were prepared and stored in the inert environment of a nitrogen drybox until ready for use. All the polymer solutions used for steady-state photophysical measurements contained ≤ 10 $\mu\text{g/ml}$ MPS-PPV to minimize the effects of concentration-dependent aggregation [7, 8, 21–23]. The fluorescence quenching experiments were performed



Scheme 2. Synthesis of TAPF.

with an MPS-PPV concentration of 5 $\mu\text{g}/\text{ml}$ (5 ppm) and quencher concentrations (MV^{2+} for aqueous solutions and TAPF in DMSO) in the sub- μM regime. We note that salt concentrations ≥ 5 mM caused MPS-PPV to precipitate from aqueous solution and that DMSO solutions of MPS-PPV appear to be stable only at salt concentrations below 10 mM. For all the Stern–Volmer quenching and fluorescence quantum yield measurements, the results were repeated on multiple sets of polymer solutions on multiple days and averaged until a standard deviation better than $\pm 7\%$ was obtained; each data point represents an average of at least 10 separate concentration-dependent PLQY experiments. To obtain Stern–Volmer quenching constants, the data were least-squares-fit to a line constrained to intersect the origin. Spectroscopic measurements showed no evidence of any ground-state electronic interaction between MPS-PPV and either TAPF or methyl viologen.

Finally, we note that both the dynamic light scattering and pump-probe transient absorption experiments required larger concentrations of MPS-PPV in order to achieve adequate signal-to-noise ratios; we typically used 100 ppm polymer solutions for transient absorption experiments and 200 ppm solutions for DLS experiments. All of the experiments reported in this paper took place at room temperature.

RESULTS AND DISCUSSION

In this section, we will first explore the photophysical properties of MPS-PPV in two different solvents, water and dimethylsulfoxide (DMSO), and then turn to study the effects of ionic strength on the electronic structure and superquenching

of MPS-PPV. What we will see is that even though the polymer chains appear to agglomerate in a similar fashion no matter what the solvent or ionic strength, the electronic structure of the chromophores along the polymer backbone depends quite sensitively on the nature of the solvent environment.

Solvent and ionic strength effects on the physical and electronic structure of MPS-PPV

Figure 3 shows the absorption (diamonds and squares) and emission (triangles and circles) spectra of dilute solutions of MPS-PPV in neat water (open symbols) and DMSO (solid symbols). The 485-nm absorption maximum, which is typical for alkoxy-substituted PPVs, is the same in both solvents, suggesting that the average conjugation length of the polymer is similar in the two solvents [8]. Figure 3 also shows that the emission spectrum of MPS-PPV is somewhat different in the two solvents, lying further to the red in water relative to DMSO. We believe that much of the apparent red-shift of the emission in water results either from solvatochromism (since water is more polar than DMSO) or from self-absorption (as much of the bluer emission in water is lost under the broader absorption band). Perhaps more important than the shape of the spectrum, however, is the fact that the photoluminescence quantum yields (PLQYs) of MPS-PPV in the two solvents are strikingly different, as reported in Table 1: the PLQY of MPS-PPV is nearly 2 orders of magnitude larger in neat DMSO (45%) than in water (0.5%). This observation is in accord with the results of Tan *et al.* [32], who found that conjugated polyelectrolytes based on sulfonated and phosphorylated PPEs were strongly fluorescent in the polar organic solvent methanol but nearly completely dark in aqueous solution. Using the fact that their charged PPEs showed a distinct absorption feature characteristic of chromophore aggregation when dissolved in

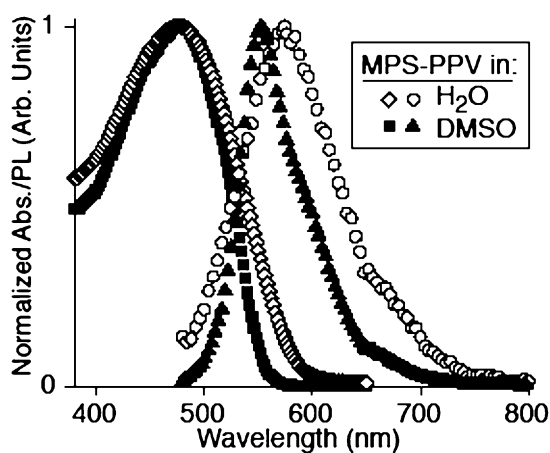


Figure 3. UV-Vis absorption (open diamonds, solid squares) and steady-state photoluminescence spectra (collected with excitation at 485 nm, open circles, solid triangles) of solutions of 5 ppm MPS-PPV in either water (open symbols) or DMSO (filled symbols).

Table 1.

Results of the DLS experiments

	Aqueous solution			DMSO solution		
	Neat	1 mM LiCl	1 mM CaCl ₂	Neat	1 mM LiCl	1 mM CaCl ₂
PLQY (%)	0.5	0.7	0.3	45	48	41
K_{SV} (M ⁻¹)	3.1×10^6	2.0×10^5	6.2×10^6	3.7×10^5	2.8×10^5	1.1×10^5
D_{hyd} (nm)	93	44	100	78	410	43

water [36], Tan *et al.* interpreted the low aqueous quantum yield as evidence of aggregation of the polyelectrolyte in water [32], so that photoexcitation leads to the formation of weakly emissive interchain species (excimers or aggregates) [7–23].

To determine whether or not a similar argument holds for the relative emission quantum yields of MPS-PPV in water and DMSO, we performed a series of dynamic light scattering (DLS) experiments to measure the size of the polymer coils in solution. Table 1 shows that the average diffusing particle diameter (twice the radius of hydration) was 93 nm in water and 78 nm in DMSO. We note, however, that previous light scattering studies of (non-charged) conjugated polymers found diameters of hydration in the range 10–25 nm for chains with molecular masses in the range of 100–1000 kDa [8, 11, 46].

Given that we expect the average molecular weight of our MPS-PPV to be ≤ 100 kDa and that there is no *a priori* reason to expect low-concentration solutions of MPS-PPV to adopt a vastly different coil shape than a similar neutral polymer, our observed MPS-PPV particle sizes are much larger than can be attributed to individual chains. Thus, our results suggest that unlike non-charged conjugated polymers, which clearly dissolve as individual chains when dilute [8, 11, 46], there is considerable agglomeration of MPS-PPV chains, even in dilute solution. This agglomeration makes sense given that the backbone of the polymer is intrinsically non-polar, so that, even with the favorable polar solvation of the charged side groups, there is a large driving force to keep the polymer backbones near each other and away from the solvent, as typical of polyelectrolytes. The fact that the size of the MPS-PPV agglomerates in water is larger than in DMSO can be rationalized simply by noting that DMSO is a better solvent for the polymer backbone than water, so that less backbone aggregation is required in DMSO.

Given that MPS-PPV chains are agglomerated in both solvents, how do we know whether or not the lower emission quantum yield of MPS-PPV in water results from increased π -electron interactions between chromophores? One of the most sensitive measures of interchain interactions is exciton–exciton annihilation (E-EA), in which neighboring excitations interact *via* Auger processes at high excitation intensities, providing a non-radiative mechanism for the destruction of excitons that does not exist at low excitation intensities. The characteristic signature of E-EA is an intensity dependence to the photophysics of conjugated polymers, with the exciton lifetime decreasing as the excitation intensity is increased [47]. Several

groups have shown that E-EA does not occur when conjugated polymer chains are isolated in dilute solution, but that it is readily observed when the chains are in contact in spin-cast films [45, 48]. We have argued that the ease with which E-EA occurs depends on the processing history of the film [7, 19], and that E-EA can even occur in solution if the polymer chains maintain a film-like environment because they are not fully dissolved [11].

Figure 4 explores the intensity-dependence of the excited-state absorption of semidilute (100 ppm) solutions of MPS-PPV in both water and DMSO. In these femtosecond pump-probe experiments, excitation was into the main exciton absorption band at 485 nm (*cf.*, Fig. 3) and the transient absorption dynamics of the excited state are probed at 800 nm. The data clearly show that the excited-state absorption persists for a much longer time in water than DMSO, suggesting that excitation of MPS-PPV in water leads to the production of long-lived, non-emissive (given the low emission quantum yield) species that are not produced when the photoexcited

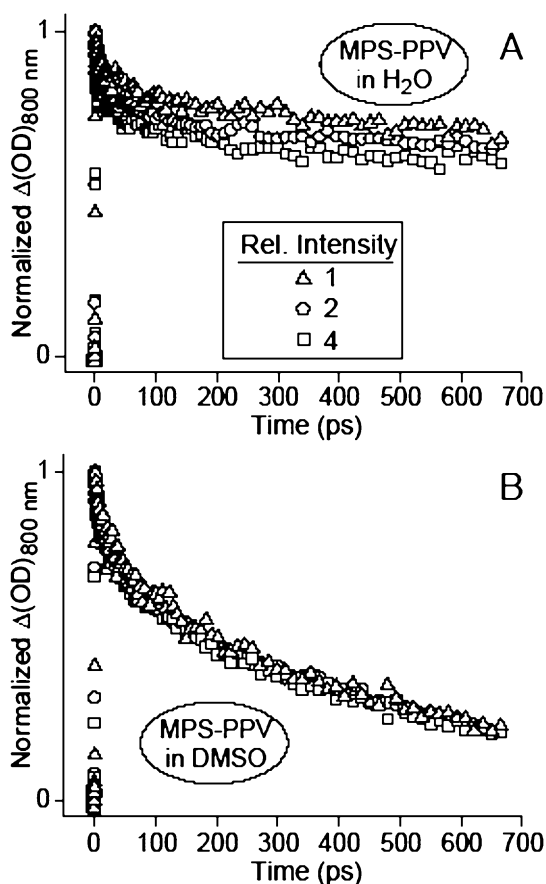


Figure 4. Transient absorption of MPS-PPV solutions in water (A) and DMSO (B) monitored at 800 nm following femtosecond excitation at 485 nm at three different excitation intensities.

polymer is dissolved in DMSO. Moreover, Fig. 4 shows that the transient dynamics are essentially independent of the excitation intensity for the DMSO solution, but that the rate of excited-state relaxation clearly increases with increasing excitation intensity for MPS-PPV dissolved in water. In combination with the presence of long-lived non-emissive species, this signature of E-EA verifies that even in dilute aqueous solutions, MPS-PPV chains are folded or interpenetrated in such a way as to allow interchain sharing of the π electrons between chromophores. Thus, the combination of the DLS data in Table 1 and the pump-probe data in Fig. 4 allows us to conclude that, even though the polymer chains agglomerate in both solvents, the chains are driven together in such a way as to cause significant interchromophore sharing of their π electrons in water but not in DMSO.

In addition to studying the properties in neat solvents, we also have investigated the effects of ionic strength and counter-ion valency on the physical and electronic structure of conjugated polyelectrolytes by adding both LiCl and CaCl₂ to solutions of MPS-PPV. At low ionic strengths (<1 mM of either salt) in either water or DMSO, the absorption and emission spectra of MPS-PPV are largely unchanged from those in the neat solvents (data not shown). Even though the addition of salt does not affect the shape of the spectrum, Table 1 shows that changing the ionic strength does have a significant effect on the polymer's PLQY. For the case of aqueous MPS-PPV, adding 1 mM LiCl increased the PLQY from 0.5% in the neat solvent to 0.7% (an increase of nearly 50%), while adding 1 mM CaCl₂ decreased the PLQY from 0.5% to 0.3% (a decrease of nearly 50%). For MPS-PPV dissolved in DMSO, the addition of salts had a much smaller effect: adding 1 mM LiCl increased the PLQY from 45% to 48%, while adding 1 mM CaCl₂ decreased the PLQY to 41%. Clearly, the addition of the salts changes the physical conformation of the polymer chains in solution, affecting both the way the chains agglomerate and the interactions between chromophores in a way that depends on the valency of the cation.

What type of changes does the addition of salt cause in the physical structure of the polyelectrolyte coils? DLS experiments, summarized in Table 1, demonstrate that addition of Li⁺ to water causes the average MPS-PPV particle size to decrease by roughly a factor of two, whereas the addition of Li⁺ to DMSO causes the MPS-PPV particle size to increase by more than a factor of five. In water, the addition of inert monovalent cations is expected to greatly diminish electrostatic interactions due to Debye screening, which in turn should lessen the mutual attractions that drive polyelectrolyte agglomeration. In contrast, we speculate that the lower dielectric constant of DMSO makes electrostatic interactions so effectively strong that all of the cations are "condensed" within the agglomerated polymer bundle [24]; in essence, by increasing the ionic strength we are beginning to "salt out" the polymer in this solvent of medium polarity, driving the chains together until the salt concentration becomes high enough to force their precipitation.

Table 1 also shows that the situation is different upon the addition of divalent cations. In water, the addition of divalent cations such as Ca²⁺ is expected

to bring polyelectrolyte chains together via a linker-mediated process, whereby like-charged polyelectrolyte chains are brought into contact *via* condensation of multivalent counterions along the polymer backbone in a “zipper” fashion [49, 50]; this type of mechanism could possibly explain the slight increase in MPS-PPV agglomerate diameter from 93 to 100 nm. The slight increase in diameter also might be explained by the higher ionic strength of the Ca^{2+} ion relative to the Li^+ cation; the Ca^{2+} cation comes closer to “salting out” the polyelectrolyte at the same salt concentration. Surprisingly, the addition of Ca^{2+} to DMSO decreased the agglomerate diameter considerably, from 78 to 43 nm. This could possibly result from the linker-mediated aggregation of chains [49, 50] if the formation of such links caused enough bending of the polymer chains to prevent large-scale agglomeration. In other words, loosely held agglomerates may be broken up by linker-driven distortions of individual pairs of chains.

Given the changes in agglomerate size, how can we explain the changes in PLQY upon the addition of salt? In water, we believe that the addition of LiCl, which decreases the coil size, helps to break up aggregated chromophores, leaving behind more isolated chromophores capable of radiative relaxation. It is also possible that in shrinking the overall agglomerate size, the ability of excitations on emissive chromophores to undergo Förster energy transfer to poorly-emissive aggregated chromophore sites is reduced: since energy migration along the backbone of conjugated polymer chains is inefficient [10], reducing the ability of chromophores to undergo through-space Förster transfer to quenching sites would lead to a significant increase in PLQY. A similar effect likely occurs when adding LiCl to DMSO, but since there were so few aggregated chromophores to begin with (*cf.*, Fig. 4), the corresponding relative increase in PLQY is much smaller. We believe that the decrease of the MPS-PPV PLQY in both solvents upon addition of CaCl_2 also results from changes in aggregation and chain conformation: it is unlikely that Ca^{2+} quenches MPS-PPV excitons by photo-induced electron transfer or any other direct mechanism. Instead, the fact that Ca^{2+} increases the agglomerate size in water suggests that its primary effect is in bringing more chromophores into inter-chain contact, or at least in bringing more chromophores within range of undergoing Förster energy transfer to a non-emissive inter-chain site during the emission lifetime. We note that previous studies of MPS-PPV for biosensing applications also have reported fluorescence quenching by addition of simple divalent salts to solution [37].

Solvent and ionic strength effects on conjugated polyelectrolyte superquenching

As mentioned in the Introduction, MPS-PPV has been the subject of extensive investigation because of its potential applications in chemo- and biosensors due to “superquenching” [30, 36–38, 40, 43]. Fluorescence quenching is typically quantified by plotting the fluorescence quantum yield as a function of quencher

concentration and fitting to the Stern–Volmer equation:

$$\frac{\Phi_0}{\Phi} = K_{SV}[Q] + 1, \quad (1)$$

where Φ_0 is the PLQY in the absence of quencher and Φ is the PLQY at a quencher concentration $[Q]$. In the low $[Q]$ regime, most such plots are linear and the slope of the line, K_{SV} , known as the Stern–Volmer constant, provides a measure of how effectively the quencher is able to reduce the emission quantum yield [44]. The effectiveness of quenching, in turn, depends both on the spatial proximity of the quencher to the fluorophore and (once the quencher is close enough) the ability of the quencher to accept an electron from or otherwise nonradiatively deactivate the fluorophore. For example, when a non-charged conjugated polymer like MEH-PPV is mixed in solution with a neutral methanofullerene derivative (which is an outstanding electron acceptor but does not form a complex with MEH-PPV), the observed K_{SV} is approx. 1000 M^{-1} [51]. However, when the conjugated polyelectrolyte MPS-PPV is mixed in solution with an oppositely-charged electron acceptor that can form a strong static complex, such as methyl viologen (MV^{2+}), K_{SV} increases to approx. 10^7 M^{-1} [37, 40]. Thus, large (i.e., $>10^6 \text{ M}^{-1}$) superquenching K_{SV} values are indicative of three things: a strong tendency for complex formation between the quencher and fluorophore, efficient excited-state electron transfer between the fluorophore and quencher, and the ability of a single quencher to harvest excitations from many neighboring fluorophores by Förster transfer [37].

Since both complex formation and the ability of excitations to migrate *via* Förster transfer will be sensitive to changes in the polymer conformation and/or degree of agglomeration, in this section we explore how the ability of MPS-PPV to undergo superquenching changes in different environments. For our studies in water, we chose MV^{2+} (*cf.*, Fig. 1) as the quencher, since Chen *et al.* have already demonstrated that this divalent species forms a strong complex with MPS-PPV capable of superquenching [37]. Unfortunately, MV^{2+} is not soluble in DMSO, so we chose the multiply-positively charged fullerene derivative TAPF as the quencher. It is well known that fullerenes readily accept electrons from conjugated polymers [5, 52], and because it is positively charged, this particular derivative is an even better electron acceptor than unfunctionalized C_{60} , as verified by cyclic voltammetry (data not shown). By choosing a multi-functionalized derivative that can be either doubly or triply charged, we also have the ability to tune the strength of complex formation between the quencher and polymer, although we will save exploration of this for future work.

Figure 5 shows Stern–Volmer plots of MPS-PPV in water (quenched by MV^{2+}) and DMSO (quenched by TAPF), both with and without added salts. Least-squares fits to the low-concentration portion of the data yield the K_{SV} values that are summarized in Table 1. The value of K_{SV} we obtain for the quenching of MPS-PPV by MV^{2+} in water, $3.1 \times 10^6 \text{ M}^{-1}$, is in satisfactory agreement with that

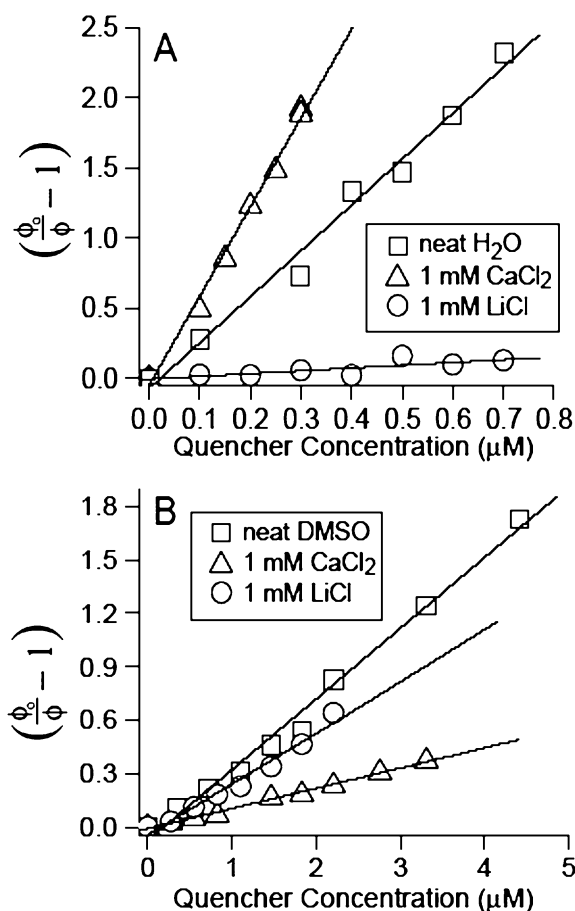


Figure 5. Stern–Volmer plots of the superquenching of MPS-PPV emission in water by MV²⁺ (A) and in DMSO by TAPF (B) with either no added salt (squares), the addition of 1 mM LiCl (triangles), or the addition of 1 mM CaCl₂.

reported previously by Chen *et al.* [37], particularly given that there appears to be some polymer batch-to-batch variability of the Stern–Volmer constant that may result from changes in the polymer molecular weight or other factors. Surprisingly, the K_{SV} for quenching of MPS-PPV by MV²⁺ in water is nearly an order of magnitude larger than the K_{SV} for quenching of MPS-PPV by TAPF in DMSO. The smaller quenching constant in DMSO might result from decreased stability of the polymer/quencher complex in DMSO relative to water or from some other effect, but whatever the cause, the observed K_{SV} of $3.7 \times 10^5 \text{ M}^{-1}$ in neat DMSO is still consistent with static quenching and complex formation.

In addition to neat water and DMSO, Fig. 5 also shows Stern–Volmer plots for the quenching of MPS-PPV in the presence of both LiCl and CaCl₂; the corresponding K_{SV} values are summarized in Table 1. Relative to neat water, the addition of 1 mM CaCl₂ doubled the effectiveness of the fluorescence quenching of MPS-PPV

by MV^{2+} , while the addition of 1 mM LiCl diminished the K_{SV} by nearly an order of magnitude. For the case of DMSO, fluorescence quenching of MPS-PPV by TAPF was less severely affected by addition of salts, but what is perhaps most striking is that the role of cation valency is reversed relative to water: the addition of $CaCl_2$ enhanced the superquenching in water but diminished the superquenching in DMSO.

How can we explain that the different counter-ions affect superquenching in different ways in the two solvents? We first consider the case of superquenching in water. We argued in the previous section that the addition of LiCl broke up inter-chain contacts and reduced agglomeration of aqueous MPS-PPV chains, leading us to expect poorer Förster coupling between chromophores. Thus, the decrease in K_{SV} for the quenching of MPS-PPV by MV^{2+} could result from the fact that each MV^{2+} can “communicate” with fewer chromophores in the presence of LiCl. Of course, the addition of LiCl might also screen the Coulomb interaction between MV^{2+} and the polymer’s sulfonate groups, so that the reduction in K_{SV} might simply be a screening effect that decreases the stability of the complex. However, screening is unlikely to be the dominant effect in the reduction of the $MV^{2+} K_{SV}$ by the addition of LiCl, given that the addition of the same concentration of $CaCl_2$, which should provide even better screening than LiCl, causes the $MV^{2+} K_{SV}$ to increase rather than decrease. Indeed, we argued in the previous section that the addition of $CaCl_2$ lead to an increase in both the agglomeration and degree of interchromophore interactions of MPS-PPV, so that the increase in K_{SV} upon addition of Ca^{2+} can be explained by an increased ability for the excitations of multiple chromophores to undergo energy migration to the site where the quencher is complexed to the polymer. Of course, this effect might be partially mitigated by screening, but it is clear that Förster transfer to the quenching site must be improved by the addition of $CaCl_2$ because there was a net increase of the K_{SV} . Overall, aqueous MPS-PPV is more luminescent in the presence of LiCl because diminished inter-chain contact frees up fluorophores otherwise aggregated in the neat solvent; the MPS-PPV fluorescence is also less efficiently quenched by MV^{2+} with added LiCl because poorer inter-chain contact prevents the Förster coupling of excitons crucial to superquenching. On the other hand, the addition of $CaCl_2$ to aqueous MPS-PPV decreases the fluorescence quantum yield relative to the neat solvent through formation of additional non-emissive inter-chain aggregates, but increases the sensitivity of MV^{2+} fluorescence quenching because aggregation of chromophores allows more excitations to migrate to complexes and be quenched, despite the fact that complex formation is likely to be weaker.

Although we can readily understand the effects of salts on the superquenching of MPS-PPV in water, interpretation of the results for MPS-PPV quenching in DMSO is somewhat more challenging. We argued in the previous section that despite the large increase in MPS-PPV chain agglomeration when LiCl is added to the polyelectrolyte in DMSO, there is little change in the amount of interchromophore contact (the PLQY actually increases slightly upon the addition of LiCl; *cf.*,

Table 1). Thus, since we do not expect the addition of LiCl to make a significant change in the ability for excitations to migrate to quenching sites, we believe that the small decrease in the ability of TAPF to quench the fluorescence of MPS-PPV in DMSO upon the addition of LiCl likely results from screening. The effect of Ca^{2+} on the fluorescence quenching of MPS-PPV by TAPF in DMSO, however, is clearly more subtle, and the mechanism must be qualitatively different than that in water. Table 1 shows that for the case of DMSO, the addition of 1 mM Ca^{2+} decreases the quenching efficiency by nearly a factor of 4. This result is surprising in that we know that addition of CaCl_2 in DMSO increases the formation of aggregated chromophores (as argued in the previous section based on the decrease of the MPS-PPV PLQY upon addition of Ca^{2+} in DMSO), but we also saw that increased chromophore aggregation led to an increase in K_{SV} for MPS-PPV in water. Again, it is possible that screening effects are more important in DMSO than water (especially given that the dielectric constant of DMSO is approx. 1/2 that of water), but the data strongly suggest that excitations on MPS-PPV in DMSO with added CaCl_2 are more easily transferred between polymer chains than without the added salt. We are continuing to explore the effects of polyvalent salts on superquenching in DMSO, and hope to present a more detailed explanation for this effect in a future publication.

CONCLUSIONS

We have shown that the conjugated polyelectrolyte MPS-PPV displays remarkably different steady-state and time-resolved photophysics in different solution environments. Fundamental properties such as the PLQY and the ability of excitations to interact and undergo E-EA are extremely sensitive to choice of solvent, emphasizing the important relationship between conjugated polymer conformation and electronic structure. Moreover, the ability of conjugated polymer chromophores to communicate *via* Förster transfer, an integral part of the superquenching phenomenon that lies at the heart of sensor applications for conjugated polyelectrolytes, depends strongly not only upon the choice of solvent but also on the ionic strength and counter-ion valency. Thus, subtle changes in the polymer conformation, caused either by changes in the environment or by the quenchers themselves can have dramatic effects on the electronic properties critical for sensor applications. Overall, our results suggest that further work must be done before extrapolating the superquenching properties of conjugated polyelectrolytes from simple aqueous solutions to *in vivo* conditions if these materials are to be exploited to their maximum potential in sensor applications.

Acknowledgements

This work was supported by the National Science Foundation under grant number DMR-0305254, and by the donors of the Petroleum Research Fund, administered by the American Chemical Society, under grant number 37029-AC5,7. S.R. was

supported as an Arthur and Mabel Beckman Foundation Undergraduate Scholar and B.J.S. is a Cottrell Scholar of Research Corporation and a Camille and Henry Dreyfus Teacher-Scholar. We thank Ignacio Martini, Fred Wudl and Yves Rubin for helpful discussions.

REFERENCES

1. R. H. Friend, R. W. Gymer, A. B. Holmes, J. H. Burroughes, R. N. Marks, C. Taliani, D. D. C. Bradley, D. A. Dos Santos, J.-L. Brédas, M. Löglund and W. R. Salaneck, *Nature* **397**, 121 (1999).
2. A. Kraft, A.C. Gramisdale and A. B. Holmes, *Angew. Chem. Int. Edn. Engl.* **37**, 402 (1998).
3. A. J. Heeger, *J. Phys. Chem. B* **105**, 8475 (2001).
4. G. Gustafsson, Y. Cao, G. M. Treacy, F. Flavetter, N. Colinari and A. J. Heeger, *Nature* **357**, 477 (1992).
5. C. J. Brabec, N. S. Sariciftci and J. C. Hummelen, *Adv. Funct. Mater.* **11**, 15 (2001).
6. J. H. Burroughes, D. D. C. Bradley, A. R. Brown, R. N. Marks, K. Mackay, R. H. Friend, P. L. Burns and A. B. Holmes, *Nature* **347**, 539 (1990).
7. T.-Q. Nguyen, I. B. Martini, J. Liu and B. J. Schwartz, *J. Phys. Chem. B* **104**, 237 (2000).
8. T.-Q. Nguyen, V. Doan and B. J. Schwartz, *J. Chem. Phys.* **110**, 4068 (1999).
9. T.-Q. Nguyen, R. C. Kwong, M. E. Thompson and B. J. Schwartz, *Appl. Phys. Lett.* **76**, 2454 (2000).
10. T.-Q. Nguyen, J. Wu, V. Doan, B. J. Schwartz and S. H. Tolbert, *Science* **288**, 652 (2000).
11. T.-Q. Nguyen, R. Y. Yee and B. J. Schwartz, *J. Photochem. Photobiol. A* **144**, 21 (2001).
12. T.-Q. Nguyen and B. J. Schwartz, *J. Chem. Phys.* **116**, 8198 (2002).
13. R. D. Schaller, J. C. Johnson, L. H. Haber, R. J. Saykally, J. Vicceli, I. Benjamin, T.-Q. Nguyen and B. J. Schwartz, *J. Phys. Chem. B* **106**, 9496 (2002).
14. R. Jakubiak, C. J. Collison, C. W. Wai, L. J. Rothberg and B. R. Hsieh, *J. Phys. Chem. A* **103**, 2394 (1999).
15. M. Yan, L. J. Rothberg, F. Papadimitrakopoulos, M. E. Galvin and T. M. Miller, *Phys. Rev. Lett.* **73**, 744 (1994).
16. M. Yan, L. J. Rothberg, E. W. Kwock and T. M. Miller, *Phys. Rev. Lett.* **75**, 1992 (1995).
17. T. G. Bjorklund, S.-H. Lim and C. J. Bardeen, *J. Phys. Chem. B* **105**, 11970 (2001).
18. S.-H. Lim, T. G. Bjorklund and C. J. Bardeen, *J. Chem. Phys.* **118**, 4297 (2003).
19. B. J. Schwartz, *Annu. Rev. Phys. Chem.* **54**, 141 (2003).
20. S. A. Jenekhe and J. A. Osaheni, *Science* **265**, 765 (1994).
21. I. D. W. Samuel, G. Rumbles, C. J. Collison, S. C. Moratti and A. B. Holmes, *Chem. Phys.* **227**, 75 (1998).
22. J. W. Blatchford, S. W. Jessen, L.-B. Lin, T. L. Gustafson, D.-K. Fu, H.-L. Wang, T. M. Swager, A. G. MacDiarmid and A. J. Epstein, *Phys. Rev. B* **54**, 9180 (1996).
23. R. Chang, J. H. Hsu, W. S. Fann, J. Yu, S. H. Lin, Y. Z. Lee and S. A. Chen, *Chem. Phys. Lett.* **317**, 153 (2000).
24. F. Oosawa, *Polyelectrolytes*. Marcel Dekker, New York, NY (1971).
25. Y. Zhang, J. F. Douglas, B. D. Ermi and E. J. Amis, *J. Chem. Phys.* **114**, 3299 (2001).
26. M. Sedláč, *Langmuir* **15**, 4045 (1999).
27. E. T. Hanson, R. Borsali and R. Pecora, *Macromolecules* **34**, 2208 (2001).
28. R. Borsali, H. Nguyen and R. Pecora, *Macromolecules* **31**, 1548 (1998).
29. S. Shi and F. Wudl, *Macromolecules* **21**, 19 (1990).
30. B. S. Gaylord, S. Wang, A. J. Heeger and G. C. Bazan, *J. Am. Chem. Soc.* **123**, 6417 (2001).
31. M. R. Pinto and K. S. Schanze, *Synthesis* **9**, 1293 (2002).

32. C. Tan, M. R. Pinto and K. S. Schanze, *Chem. Commun.*, 446 (2002).
33. M. R. Pinto, B. M. Kristal and K. S. Schanze, *Langmuir* **19**, 6523 (2003).
34. J.-S. Yang and T. M. Swager, *J. Am. Chem. Soc.* **120**, 5231 (1998).
35. J.-S. Yang and T. M. Swager, *J. Am. Chem. Soc.* **120**, 11864 (1998).
36. D. T. McQuade, A. E. Pullen and T. M. Swager, *Chem. Rev.* **100**, 2537 (2000).
37. L. Chen, D. W. McBranch, H.-L. Wang, R. Helgeson, F. Wudl and D. G. Whitten, *Proc. Natl. Acad. Sci. USA* **96**, 12287 (1999).
38. L. Chen, S. Xu, D. McBranch and D. Whitten, *J. Am. Chem. Soc.* **122**, 9302 (2000).
39. C. Fan, K. W. Plaxco and A. J. Heeger, *J. Am. Chem. Soc.* **124**, 5642 (2002).
40. D. Wang, J. Wang, D. Moses, G. Bazan, A. J. Heeger, J.-H. Park and Y.-W. Park, *Synth. Met.* **119**, 587 (2001).
41. N. DiCesare, M. R. Pinto, K. S. Schanze and J. R. Lakowicz, *Langmuir* **18**, 7785 (2002).
42. D. Wang, J. Lal, D. Moses, G. Bazan and A. J. Heeger, *Chem. Phys. Lett.* **348**, 411 (2001).
43. L. Chen, D. McBranch, R. Wang and D. Whitten, *Chem. Phys. Lett.* **330**, 27 (2000).
44. J. R. Lakowicz, *Principles of Fluorescence Spectroscopy*, 2nd edn. Kluwer Academic/Plenum, New York, NY (1999).
45. I. B. Martini, A. D. Smith and B. J. Schwartz, *Phys. Rev. B* **69**, 35205 (2004).
46. C. L. Gettinger, A. J. Heeger, J. M. Drake and D. J. Pine, *J. Chem. Phys.* **101**, 1673 (1994).
47. R. G. Kepler, V. S. Valencia, S. J. Jabos and J. J. McNamara, *Synth. Met.* **78**, 227 (1996).
48. B. Kraabel, V. I. Klimov, R. Kohlman, S. Xu, H.-L. Wang and D. W. McBranch, *Phys. Rev. B* **61**, 8501 (2000).
49. I. Borukhov, R. F. Bruinsma, W. M. Gelbart and A. J. Liu, *Phys. Rev. Lett.* **86**, 2182 (2001).
50. I. Borukhov, K.-C. Lee, R. F. Bruinsma, W. M. Gelbart, A. J. Liu and M. J. Stevens, *J. Chem. Phys.* **117**, 462 (2002).
51. J. Wang, D. Wang, D. Moses and A. J. Heeger, *J. Appl. Polym. Sci.* **82**, 2553 (2001).
52. N. S. Sariciftci, L. Smilowitz, A. J. Heeger and F. Wudl, *Science* **258**, 1474 (1992).